
Modelling a 3D Rainwater Droplet in a Strong Electric Field

Dirk Langemann¹

University of Rostock, department of mathematics, Universitätsplatz 1, 18051 Rostock, Germany dirk.langemann@mathematik.uni-rostock.de

Summary. Outdoor high-voltage equipment is exposed to moisture, rain and pollution. Water droplets on insulators influence negatively the material-aging process. A numerical procedure is presented which simulates the droplet behavior in a strong electric field. It consists in an iteration over an electric and a mechanical sub-problem to solve a coupled system of boundary value problems on the free domain of the droplet. Finally we give the resulting droplet shapes for 2D and 3D models, and we mention the behavior of a droplet in an inhomogeneous electric field.

1 Introduction to the Coupled Problem

The question of the behavior of the droplet in an electric field is a feed-back problem. The droplet shape determines the ponderomotoric force density p_e caused by the electric field, and thus the electric field changes the equilibrium of forces at the droplet surface and influences the droplet shape. The mechanical sub-problem of the droplet shape and the electric sub-problem of finding p_e are decoupled via an iteration in Sect. 2. After evolving both sub-problems stationary 3D and 2D results are given in Sect. 5. The problem is extended to non-stationary droplets in inhomogeneous electric fields in Sect. 6.

The experimentally observed droplets [6, 13] become lengthened and flattened, they oscillate with double the frequency of an applied alternating voltage and their changes are visible by naked eyes. A model of the experimental set-up [6] is shown in Fig. 1. A conductive water droplet of $V = 50\mu\text{l}$ lays on a solid support made of resin which contains two electrodes with the applied voltage of $2U$ between them. The upper surface Γ_u describes the droplet shape. The outer normal relating to the droplet is called \mathbf{n} .

2 Decoupling Strategy

The two basic sub-problems of the coupled problem are the electric \mathcal{P} -problem and mechanical \mathcal{R} -problem. The \mathcal{P} -problem consists in finding the outer force

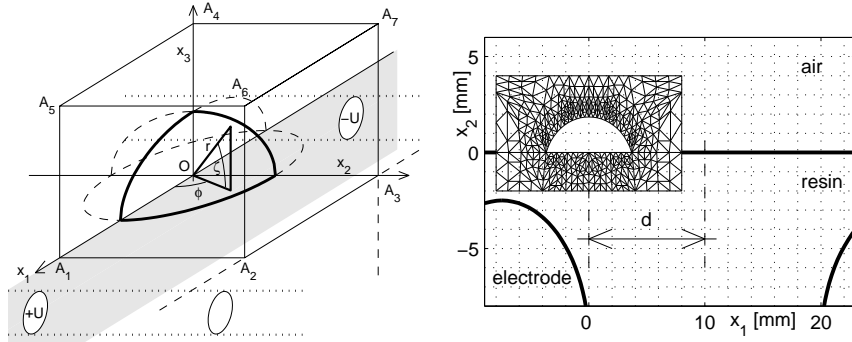


Fig. 1. (a) Experimental set-up. The bold lines mark the quarter droplet laying on the surface $OA_1A_2A_3A_4$ which coincides with the (x_1, x_2) -plane. (b) 2D intersection through a set-up with non-centered droplet. FE/FD discretization scheme.

density p_e for a given Γ_u which is parameterized by spherical co-ordinates $r(\varphi, \zeta)$, cf. Fig. 1 (a). The \mathcal{R} -problem is the search for Γ_u depending on p_e . In Sect. 4.1 the force density p_e is assigned to the unknown Γ_u . The sub-problems are expressed by the operators $\mathcal{P} : \Gamma_u \rightarrow p_e$ and $\mathcal{R} : p_e \rightarrow \Gamma_u$. In this formalism, we search for a fixed point $\Gamma_u^{\text{fix}} = \mathcal{R}\mathcal{P}\Gamma_u^{\text{fix}}$ described by r^{fix} by a Banach-like iteration [1, 14] with a relaxation ω , i.e.

$$r^{(k+1)} = \omega \mathcal{R}\mathcal{P}r^{(k)} + (1 - \omega)r^{(k)} \quad \text{with} \quad \lim_{k \rightarrow \infty} r^{(k)} = r^{\text{fix}}. \quad (1)$$

3 The Electric \mathcal{P} -Sub-Problem

This section deals with the boundary value problem for the stationary potential Φ , its numerics and the determination of the force density p_e .

3.1 The Stationary Electric Field Around the Droplet

The support Ω of the electric field is the resin, $\varepsilon_{\text{res}} = 4$, and the air. For formal simplification we write $\varepsilon(\mathbf{x}) = \varepsilon_{\text{res}}$ for $\mathbf{x} \in \Gamma_s$ and $\varepsilon(\mathbf{x}) = \varepsilon_{\text{air}}$ on Γ_u . Rainwater is conductive, and the droplet is free of charge. We get the linear elliptic boundary value problem with Dirichlet-conditions at the electrodes Γ_e

$$\begin{aligned} \nabla \cdot [\varepsilon(\mathbf{x}) \nabla \Phi(\mathbf{x})] &= 0 \quad \text{in } \mathbf{x} \in \Omega, \\ \Phi(\mathbf{x}) &= \pm U \quad \text{on } \mathbf{x} \in \Gamma_e, \\ \Phi(\mathbf{x}) &= c \quad \text{on } \mathbf{x} \in \Gamma_u \cup \Gamma_s, \end{aligned} \quad (2)$$

$$\int_{\Gamma_u \cup \Gamma_s} \varepsilon(\mathbf{x}) \frac{\partial}{\partial \mathbf{n}} \Phi(\mathbf{x}) \, d\mathbf{x} = 0.$$

The integral over the density of free charge in (2) determines the constant c . The potential vanishes at infinity and has a finite energy. The boundary value (2) is linear for fixed Ω , but Ω depends on the searched droplet shape.

The electric field is $\mathbf{E}(\mathbf{x}) = -\nabla\Phi(\mathbf{x})$ and the dielectric displacement is $\mathbf{D}(\mathbf{x}) = \varepsilon_0\varepsilon(\mathbf{x})\mathbf{E}(\mathbf{x})$. The Maxwell stress tensor and the ponderomotoric surface force density are [2, 5]

$$\mathbb{T} = \mathbf{E}\mathbf{D}^T - \frac{1}{2}(\mathbf{E}^T\mathbf{D})I \quad \text{and} \quad p_e(\mathbf{x}) = \mathbb{T}^+(\mathbf{x})\mathbf{n} = \frac{1}{2}\varepsilon_0\varepsilon(\mathbf{x}) \left(\frac{\partial\Phi(\mathbf{x})}{\partial\mathbf{n}} \right)^2 \mathbf{n}$$

with the unilateral limit $\mathbb{T}^+(\mathbf{x})$ of the stress tensor at the droplet surface.

3.2 Numerics of the Electric Sub-Problem

The numerical solution of (2) requires some carefulness. Finite differences or finite integration techniques [12] approximate well the potential Φ , but the outer force density p_e depending on $\nabla\Phi$ cannot be evaluated on the curved surface outside the meshes in satisfactory accuracy. Boundary element methods are ineffective due to the non-constant dielectric constant $\varepsilon(\mathbf{x})$. Finite elements in whole the 3D domain do not justify the costly effort to find p_e on the droplet surface only.

Thus, we use a combination of finite elements on an adapted tetrahedral grid refined near $\Gamma_u \cup \Gamma_s$ in a parallelepiped around the droplet and finite differences remote from it. A sketch of the hybrid discretization scheme is given in Fig. 1 (b).

The numerical errors in the finite element approximation of Φ and $\nabla\Phi$ are small, and they do so for p_e . Any local disturbances caused by the finite differences outside the parallelepiped – e.g. on the curved Γ_e – are levelled out in its neighborhood, and they do not perturbate p_e . The computational costs are restricted. In the examples, a tetrahedral grid with 150,000 elements was used which could be handle on a standard desktop computer.

3.3 Scattered p_e -Data on the Droplet Surface

The extrapolation of the p_e data found by the finite element computation onto whole the droplet surface occurs in particular in three-dimensional models. A relatively small number of tetrahedral elements borders on the two-dimensional Γ_u . Their indices are collected in J and the outer force density $p_e(\mathbf{x}_r^{(j)})$ is known in their centres $\mathbf{x}_r^{(j)}$, $j \in J$

For solving the \mathcal{R} -problem, the outer force density p_e is required at mesh-points \mathbf{y}_r of a fixed (φ, ζ) -grid. The tetrahedral grid is adapted to the changing surface Γ_u in each step of the iteration (1) and thus the points $\mathbf{x}_r^{(j)}$ do not have fixed (φ, ζ) -co-ordinates. All points $\mathbf{x}_r^{(j)}$ lay inside Γ_u . An extrapolation should continue p_e reasonably to whole the surface Γ_u . Therefore we use the weighted average [4]

$$p_e(\mathbf{y}_r) = p_e^{\text{out}}(\mathbf{y}_r) + \left[\sum_{j \in J} \gamma(\mathbf{x}_r^{(j)}, \mathbf{y}_r) \right]^{-1} \sum_{j \in J} \gamma(\mathbf{x}_r^{(j)}, \mathbf{y}_r) p_e(\mathbf{x}_r^{(j)})$$

with a decreasing function γ of the distance between $\mathbf{x}_\Gamma, \mathbf{y}_\Gamma \in \Gamma_u$ and a corrector term $p_e^{\text{out}}(\mathbf{y}_\Gamma)$ containing the known asymptotic behavior of the outer force density near the triple line $\partial\Gamma_u$ with $\zeta = 0$. An homogenization [11] near the triple line and an expansion in series yield

$$p_e(\mathbf{y}(\varphi, \zeta)) \sim \zeta^{2(a-1)} \text{ for } \zeta \rightarrow 0 \text{ and all } \varphi \quad (3)$$

with the smallest positive $a \approx 0.54$ in $\varepsilon_{\text{res}} \tan(a(\pi - \vartheta)) = -\varepsilon_{\text{air}} \tan(a\pi)$ [7] and the contact angle $\vartheta = 1.1$. The relation (3) assures the non-existence of an essential concentration of free charge and thus of forces on $\partial\Gamma_u$.

4 The Mechanical \mathcal{R} -Sub-Problem

The counterpart to the electric sub-problem is the \mathcal{R} -problem where the droplet shape Γ_u is searched for a given outer force density p_e .

4.1 The Non-Linear Boundary Value Problem on the Droplet

The force densities acting on Γ_u are the capillary pressure $p_k(\mathbf{x})$, the hydrostatic pressure $p_h(\mathbf{x}) + p_0$ and the outer force density $p_e(\mathbf{x})$ caused by the electric field. The capillary pressure is given by the Young-Laplace-equation

$$p_k(\mathbf{x}) = -2\sigma\kappa(\mathbf{x})\mathbf{n}$$

with the mean curvature $\kappa(\mathbf{x}) \geq 0$ of the droplet surface. The hydrostatic pressure p_h depends on the height of the droplet. With the mass density ϱ and the gravitational acceleration g we get

$$p_h(\mathbf{x}) = g\varrho \left(\max_{\mathbf{x} \in \Gamma_u} x_3 - x_3 \right) \mathbf{n}.$$

The incompressibility of the water yields the Lagrangian multiplier p_0 . The equilibrium of forces leads to a boundary value problem

$$p_e(\mathbf{x}) + p_k(\mathbf{x}) + p_h(\mathbf{x}) + p_0 = 0 \quad (4)$$

with the boundary conditions of a constant contact angle ϑ on $\partial\Gamma_u$. The problem (4) is formulated on the free Γ_u but the parameterization maps it to the fixed (φ, ζ) -domain $\varphi \in [0, 2\pi)$ and $\zeta \in [0, \pi/2]$.

4.2 Numerics of the Mechanical Sub-Problem

The parameterization $\mathbf{x} = \mathbf{x}(\varphi, \zeta)$ generates a bijective map $\Gamma_u \leftrightarrow \Gamma'_u$ between variable surfaces Γ_u and Γ'_u . The given outer force p_e is assigned to (φ, ζ) . In opposite the force densities p_k and p_h depend on Γ_u , and they can be expressed directly for every occurring surface.

Let τ be an auxiliary time. We simulate a transient process of a damped droplet deformation by the evolution problem

$$\frac{\partial}{\partial \tau} r(\varphi, \zeta, \tau) = p_e(\varphi, \zeta) + p_k(\varphi, \zeta, \tau) + p_h(\varphi, \zeta, \tau) + p_0(\tau) \quad (5)$$

with the boundary condition of a fixed contact angle ϑ and nearly arbitrary initial conditions. The limit solution $r_{\text{lim}}(\varphi, \zeta) = \lim_{\tau \rightarrow \infty} r(\varphi, \zeta, \tau)$ of the parabolic system (5) is the solution of the non-linear elliptic boundary value problem (4). Cause of $p_0(\tau)$ we solve a differential-algebraic system. The limit solution is found with small numerical costs within $\tau < 1$ ms.

If $p_0(\tau)$ is replaced by a penalty force assuring an incompressible droplet volume V [9], the discretized problem (5) becomes a system of stiff ordinary differential equations [3].

5 Results in 3D Compared with the 2D Case

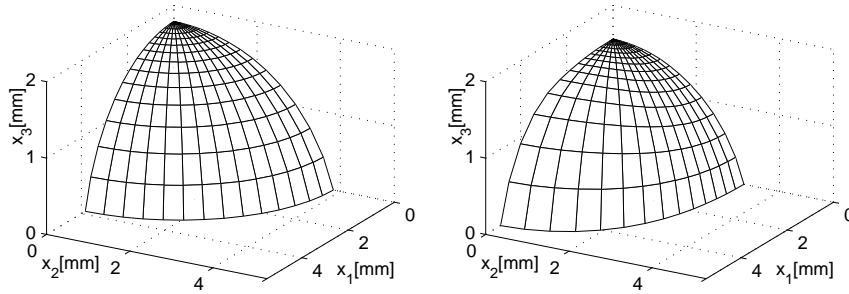


Fig. 2. (a) Quarter droplets in the absence of an electric field and (b) in a strong electric field, $U = 24$ kV. Plots are not true in scale, height is exaggerated.

Figure 2 (a) shows a quarter droplet in the absence of an electric field. It is axial-symmetric. After the application of a strong electric field, it becomes lengthened and flattened, Fig. 2 (b). The width diminishes.

This effects is illustrated by the ground patches in Fig. 3 together with the measurements of the droplets. The droplet height is independent of sign U . Hence a droplet in a low frequent alternating electric field oscillates with twice the frequency [7, 13].

Figure 4 gives the respective 2D results for comparison. The difference between conductive and dielectric droplets is discussed in [8]. 2D droplet models react more sensitive on an applied field. The 2D model lacks the second curvature term, and the incompressibility of the fluid couples length and height of a 2D droplet model in an enforced manner [9].

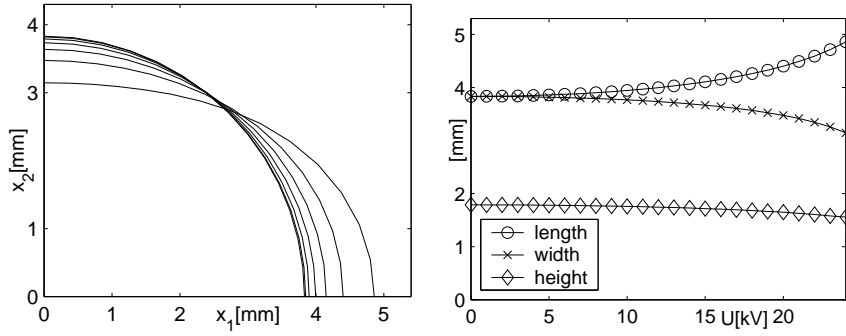


Fig. 3. (a) Quarter ground patches of 3D droplets for $U = 0, 4, \dots, 20, 24$ kV from above. (b) Heights, widths and lengths of $50 \mu\text{l}$ -droplets depending on U .

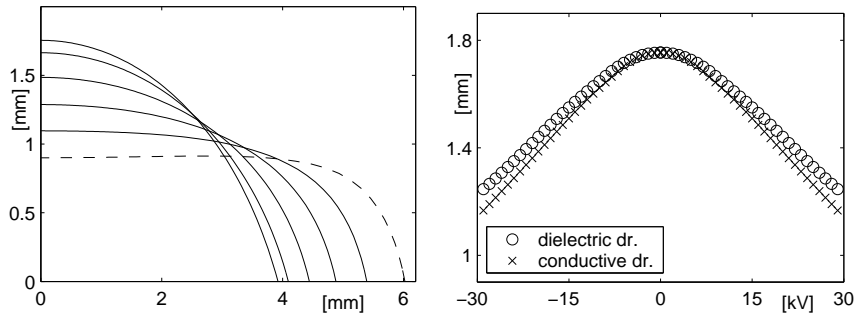


Fig. 4. (a) 2D droplet shapes for $U = 0, 8, 16, 32$ kV and a droplet being torn up by 40 kV in dashed line. (b) Heights of conductive and dielectric 2D droplets depending on U

6 Moving Droplets – Droplets in Inhomogeneous Fields

The integral over the ponderomotive force density p_e is not necessarily vanishing. In general the droplet suffers a total force \mathbf{F} and moves leaving a water film. Without real charge and for $\varepsilon(\mathbf{x}) = 1$, we show analytically that

$$\lim_{V \rightarrow 0} \frac{\mathbf{F}(\bar{\mathbf{x}})}{V} = \varepsilon_0 \nabla \left| \nabla \tilde{\Phi}(\bar{\mathbf{x}}) \right|^2 = 2\varepsilon_0 \nabla \tilde{\mathbf{E}}(\bar{\mathbf{x}}) \cdot \tilde{\mathbf{E}}(\bar{\mathbf{x}})$$

holds with the undisturbed electric potential $\tilde{\Phi}$ in the absence of the droplet and with the droplet's centre of gravity $\bar{\mathbf{x}}$ [10]. The case $\mathbf{F} = 0$ is the rather extraordinary one, e.g. if $\tilde{\mathbf{E}}$ is perfectly homogeneous or if the particle is dimensionless $V = 0$. In the experimental set-up the horizontal component of \mathbf{F} vanishes only in the symmetric position $\bar{x}_1 = 0$.

The deformation of the droplet runs much faster than the motion of the droplet as a whole. We separate the total motion $\bar{\mathbf{x}}(t)$ from the deformation by an additional Lagrangian multiplier $-\mathbf{f}$ in Eq. (4) counteracting \mathbf{F}

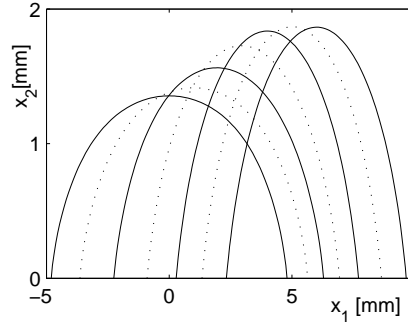


Fig. 5. Droplet shapes for different displacements $\bar{x}_1 = 0, 4, \dots, 24$ mm.

$$p_e(\mathbf{x}) + p_k(\mathbf{x}) + p_h(\mathbf{x}) + p_0 - \mathbf{f} = 0. \quad (6)$$

Figure 5 shows 2D droplets at different positions \bar{x}_1 . Outside the symmetric centre the flattening and lengthening effect of the electric field is smaller [10].

In a first attempt, the total motion $\mathbf{x}(t)$ of the droplet is governed by one equation of motion of the form

$$\rho V \ddot{\mathbf{x}}(t) = \mathbf{F}(\bar{\mathbf{x}}) - \mathbf{F}_{cf}(\bar{\mathbf{x}}, \dot{\bar{\mathbf{x}}}, \mathbf{F}).$$

The constrained and frictional forces are collected in \mathbf{F}_{cf} . The droplets move into the maxima of the energy $\tilde{\mathbf{E}}(\mathbf{x})^T \tilde{\mathbf{D}}(\mathbf{x})/2$ of the undisturbed field, Fig. 6. Simulating the droplet motion precisely would require an extension of ansatzes like [15] and a study of the adhesion between rainwater and resin.

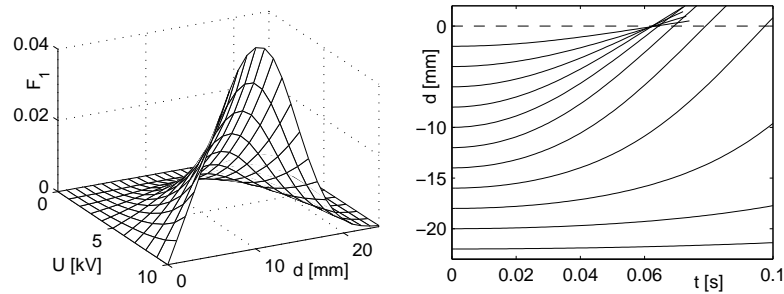


Fig. 6. (a) Horizontal part of \mathbf{F} (2D in N/m) depending on $d = \bar{x}_1$ and U . (b) Trajectories of the droplet as a whole with different initial conditions.

7 Conclusion

An algorithm was presented which enables us to simulate the droplet behavior in strong electric fields in 3D and 2D. It concentrates on the effects on the

droplet surface. Particular features of the 3D simulations are the restriction of the finite element approximation to a domain close to the droplet and an extrapolation of the discretized ponderomotive force density on the droplet surface.

The observation of moving droplets in non-homogeneous electric fields motivates a forthcoming hydrodynamical investigation of the droplet fluid including adhesion to the material of the support.

A further challenge in the simulation of the droplet behavior is the consideration of specific surface properties of aging insulating material.

References

1. Frischmuth, K., Hänler, M.: Numerical analysis of the closed osmometer problem. *ZAMM* **79** (2), 107–116 (1999)
2. Greiner, W.: *Classical Electrodynamics*. Springer, New York (1998)
3. Hairer, E., Wanner, G.: *Solving Ordinary Differential Equations. Part 2. Stiff and Differential-Algebraic Problems*. Springer, Berlin (1991)
4. Iske, A., Quak, E., Floater, M.S.: *Tutorials on Multiresolution in Geometric Modelling*. Springer, Berlin (2002)
5. Jackson, J.D.: *Classical Electrodynamics*. Wiley, New York (1999)
6. Keim, S., König, D.: Study of the behavior of droplets on polymeric surfaces under the influence of an applied electrical field. In: *Proceedings of the IEEE Conference on Electrical Insulation and Dielectric Phenomena*, Austin. 707–710 (1999)
7. Langemann, D.: A droplet in a stationary field. *Mathematics and Computers in Simulation* **63** (6) 529–539 (2003)
8. Langemann, D.: The free transmission problem for a water droplet. In: *Proceedings of the 4th International Conference on Large-Scale Scientific Computing*, Sozopol, Bulgaria. Springer, Berlin 387–395 (2004)
9. Langemann, D., Krüger, M.: 3D model of a droplet in an electric field. *Mathematics and Computers in Simulation* **66** (6) 539–549 (2004)
10. Langemann, D.: Modelling a droplet moving in an electric field. *Mathematics and Computers in Simulation*. Submitted (2004)
11. Mazja, V.G., Nazarov, S.A., Plamenevskij, B.A.: *Asymptotic Theory of Elliptic Boundary Value Problems in Singularly Perturbed Domains*. Birkhäuser, Basel (2000)
12. van Rienen, U., Clemens, M., Wendland, T.: Simulation of Low-Frequency Fields on Insulators with Light Contaminations. *IEEE Trans, Magn.* **32** (3) 816–819 (1996)
13. Schreiber, U., van Rienen, U.: Simulation of the behavior of droplets on polymeric surfaces under the influence of an applied electrical field. In: *Proceedings of the 9th Biennial IEEE Conference CEFEC*, Milwaukee (2000)
14. Sethian, J.A.: *Level Set Methods: Evolving Interfaces In Geometry, Fluid Mechanics, Computer Vision and Material Science*. Cambridge Univ. Press, Cambridge (1998)
15. Taylor, G.I.: The circulation produced in a drop by an electric field. In: *Proceedings of the Royal Society, A* **291** 159–166 (1966)